

# The Gas-Phase Equilibrium Structures of $\text{Si}_8\text{O}_{12}(\text{OSiMe}_3)_8$ and $\text{Si}_8\text{O}_{12}(\text{CHCH}_2)_8$

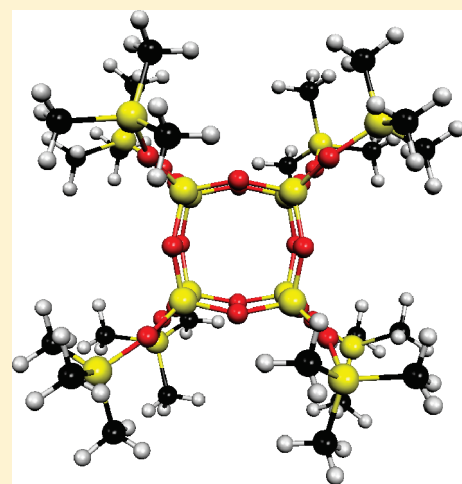
Derek A. Wann,<sup>\*,†</sup> Christopher N. Dickson,<sup>†</sup> Paul D. Lickiss,<sup>\*,‡</sup> Heather E. Robertson,<sup>†</sup> and David W. H. Rankin<sup>†</sup>

<sup>†</sup>School of Chemistry, University of Edinburgh, West Mains Road, Edinburgh, UK EH9 3JJ

<sup>‡</sup>Department of Chemistry, Imperial College London, South Kensington, London, UK SW7 2AZ

**S** Supporting Information

**ABSTRACT:** The equilibrium molecular structure of  $\text{Si}_8\text{O}_{12}(\text{OSiMe}_3)_8$  has been determined in the gas phase by electron diffraction (GED). With OSi-containing substituents on the cage silicon atoms, this molecule contains a moiety, which would, if reproduced in a periodic manner, yield a zeolite-type structure. Extensive *ab initio* calculations were used to identify two conformers of this molecule, with  $D_4$  and  $D_2$  point-group symmetries; the  $D_4$ -symmetric conformer was approximately  $1.2 \text{ kJ mol}^{-1}$  lower in energy. With 132 atoms in each conformer, this is one of the largest studies to be undertaken using gas electron diffraction. Semiempirical molecular-dynamics (SE-MD) calculations were used to give amplitudes of vibration, vibrational distance corrections (differences between interatomic distances in the equilibrium structure and the vibrationally averaged distances that are given directly by the diffraction data), and anharmonic constants. The structure of  $\text{Si}_8\text{O}_{12}(\text{CHCH}_2)_8$  has also been determined by GED. Calculations showed that the vinyl groups are fairly unhindered and rotate between three minimum-energy positions. Ultimately, all possible combinations of the vinyl groups in these low-energy positions were accounted for in the GED model.



## INTRODUCTION

The chemistry of polyhedral silsesquioxanes has been the subject of increasing interest in recent years, with particular focus on the cubic octasilsesquioxanes of general formula  $\text{Si}_8\text{O}_{12}\text{R}_8$ , which have found many applications in, for example, nanocomposites and biomaterials.<sup>1,2</sup> Two compounds that are finding increasing use as precursors to novel materials are  $\text{Si}_8\text{O}_{12}(\text{OSiMe}_2\text{H})_8$ , which readily undergoes a wide range of hydrosilylation reactions, and  $\text{Si}_8\text{O}_{12}(\text{CHCH}_2)_8$ , which has been shown to take part in many addition and metathesis reactions.<sup>1,2</sup> The closely related but incompletely condensed silsesquioxanes,  $\text{Si}_7\text{O}_9\text{R}_7(\text{OH})_3$ , have also been studied extensively, as they can react with organometallic precursors to give useful models for catalysts on silica surfaces.<sup>3–5</sup> The increasing interest in these types of compounds is leading to more fundamental studies on the nature of silsesquioxane polyhedra, both experimentally and computationally.<sup>1,2,6</sup> Gas-phase studies allow the structures of the polyhedra to be determined in the absence of crystal packing forces, which have been found to cause significant deformations of the (ideally) regular silsesquioxane polyhedra.<sup>1,2</sup>

The current study of  $\text{Si}_8\text{O}_{12}(\text{OSiMe}_3)_8$  [which, being more symmetrical than  $\text{Si}_8\text{O}_{12}(\text{OSiMe}_2\text{H})_8$ , greatly aids the analysis of gas electron diffraction data] provides the second gas-phase experimental determination of the structure of a silsesquioxane with only oxygen atoms bonded to silicon. The first was

$\text{Si}_6\text{O}_9(\text{OSiMe}_3)_6$ ,<sup>7</sup> which is related to the silicate anion,  $[\text{Si}_6\text{O}_{15}]^{6-}$ , and potentially to a zeolite structure containing six- and eight-membered rings, although zeolites with such structures have not yet been synthesized. However, the gas-phase determination of the structure of  $\text{Si}_8\text{O}_{12}(\text{OSiMe}_3)_8$  provides the first experimentally determined structure of the related cubic  $[\text{Si}_8\text{O}_{20}]^{8-}$  unit, which is a much more significant structural motif in zeolites. Thus, the gas-phase structure of a single molecular species containing the cubic building block is not affected by lattice or solvent effects and may be regarded as a model for units building up solid structures.

As with the determinations of experimental equilibrium structures for other silsesquioxanes,<sup>8–10</sup> molecular-dynamics simulations have been used to predict vibrational quantities required for use in the gas electron diffraction (GED) refinement.

The structure of the related molecule  $\text{Si}_8\text{O}_{12}(\text{CHCH}_2)_8$  has also been determined. Unlike  $\text{Si}_8\text{O}_{12}(\text{OSiMe}_3)_8$ , for which calculations indicated that two distinct conformations would be present in the experimental sample,  $\text{Si}_8\text{O}_{12}(\text{CHCH}_2)_8$  was predicted to exist as a mixture of all possible conformers, and the data were modeled to account for this.

Received: December 8, 2010

## EXPERIMENTAL SECTION

**Preparation of  $\text{Si}_8\text{O}_{12}(\text{OSiMe}_3)_8$  and  $\text{Si}_8\text{O}_{12}(\text{CHCH}_2)_8$ .** The trimethylsiloxy and vinyl silsesquioxanes are readily prepared by silylation of  $[\text{Si}_8\text{O}_{20}]^{8-11}$  and hydrolysis of  $\text{Cl}_3\text{SiCHCH}_2$ ,<sup>12</sup> respectively. However, the samples used in this electron-diffraction study were purchased from Hybrid Plastics, Inc. and used without further purification.

**Computational Studies.** Previous geometry optimizations for silsesquioxanes have shown that the inclusion of polarization functions in the basis set is important for an accurate description of the Si–O bond lengths.<sup>8,10</sup> These studies also showed that MP2 and DFT calculations using the B3LYP functional produce similar results for POSS compounds. Geometry optimizations for  $\text{Si}_8\text{O}_{12}(\text{OSiMe}_3)_8$  were therefore performed (using the Gaussian 03 suite of programs<sup>13</sup> and the resources of the EPSRC National Service for Computational Chemistry Software<sup>14</sup>) using both the 6-31G\* and 6-311G\* basis sets<sup>15,16</sup> with the B3LYP functional.<sup>17–19</sup> Ideally, larger basis sets such as 6-311++G-(3df,3dp) would have been used, but this was too computationally demanding for such a large molecule.

As gas electron diffraction (GED) experiments yield time-averaged structures in which the effects of vibrations may distort the equilibrium geometry of the structure, it is common to calculate corrections to apply to the distances, thereby giving more accurate comparisons between experimental and theoretical structures. In this study, the molecular dynamics (MD) method<sup>8</sup> of obtaining distance corrections, amplitudes of vibration, and anharmonic constants has been used.

When studying the related POSS structure  $\text{Si}_6\text{O}_9(\text{OSiMe}_3)_6$ ,<sup>7</sup> we found that employing plane-wave DFT-MD was prohibitively expensive and instead opted to perform semiempirical molecular-dynamics (SE-MD) simulations. That study involved performing geometry optimizations at a number of levels of theory, and we found that PM6<sup>20</sup> and MNDO/D<sup>21</sup> reproduced the Si–O amplitudes of vibration and other structural parameters most accurately. As the system studied in this work is larger than any studied before, it was reasonable to assume that DFT-MD would also prove too expensive, and so SE-MD simulations were run. The PM6 methodology was chosen on the basis of the conclusions of these previous works, as the amplitudes of vibration are slightly more reliable than those given by MNDO/D.

All SE-MD simulations were performed using the CP2K code<sup>22</sup> and the resources of the EaStCHEM Research Computing Facility.<sup>23</sup> A geometry optimization was initially performed using the PM6 method, followed by an SE-MD simulation in the NVT ensemble. The canonical sampling via velocity rescaling (CSVR) thermostat<sup>24</sup> was used to regulate the system to the experimental temperature of 500 K. The simulation was run for a total of 30 ps with a time step of 0.5 fs.

Following the completion of the molecular-dynamics simulations, amplitudes of vibration, distance corrections, and anharmonic constants were determined using MDSIM v0.4.0,<sup>25</sup> which computes this information from the calculated equilibrium geometry and the many interatomic distances assumed by each atom pair during the MD simulation.

Geometry optimizations of  $\text{Si}_8\text{O}_{12}\text{H}_{8-n}(\text{CHCH}_2)_n$  ( $n = 1, 2, 8$ ) were initially performed for various conformations (using the Gaussian 03 suite of programs<sup>13</sup> and the resources of the EPSRC National Service for Computational Chemistry Software)<sup>14</sup> using both the 3-21G\* and 6-31G\* basis sets with the HF method. For the high symmetry  $D_4$  conformer, a calculation was performed at the B3LYP/6-311++G-(3df,3pd) level, which has been shown in previous studies<sup>7–10</sup> to give accurate structures.

A frequency calculation (RHF/6-31G\*) for  $\text{Si}_8\text{O}_{12}(\text{CHCH}_2)_8$  was performed to give a set of force constants, to be used with the SHRINK program<sup>26</sup> to get estimates of the amplitudes of vibration and distance corrections for use in the GED refinements. These values were not expected to be very accurate in themselves, but they were the best data available to use at the start of the refinement.

**Gas Electron Diffraction.** Data were collected for  $\text{Si}_8\text{O}_{12}(\text{OSiMe}_3)_8$  and  $\text{Si}_8\text{O}_{12}(\text{CHCH}_2)_8$  using the Edinburgh GED apparatus<sup>27</sup> with an accelerating voltage of 40 kV (equivalent to an electron wavelength of approximately 6.0 pm). Each experiment was performed at two different nozzle-to-film distances to maximize the range of scattering data available. The scattering intensities were recorded on Kodak Electron Image films; nozzle-to-film distances and nozzle and sample temperatures are given in Table S1 (Supporting Information). The camera distances were calculated using diffraction patterns of benzene recorded immediately after each of the sample runs. The scattering intensities were measured using an Epson Expression 1680 Pro flat-bed scanner and converted to mean optical densities using a method described elsewhere.<sup>28</sup> The data were then reduced and analyzed using the ed@ed least-squares refinement program v3.0,<sup>29</sup> employing the scattering factors of Ross et al.<sup>30</sup> The weighting points for the off-diagonal weight matrix, correlation parameters, and scale factors are shown in Table S1 (Supporting Information).

The GED refinement procedure used here for  $\text{Si}_8\text{O}_{12}(\text{OSiMe}_3)_8$  gives interatomic distances that we have termed  $r_{e,\text{MD}}$ , indicating that corrections of the form  $r_a - r_e$  have been determined from the PM6 SE-MD simulations described above. The calculated amplitudes of vibration used as starting values in the refinement were also taken from MD simulations (and are termed  $u_{\text{MD}}$ ), as were anharmonic constants applied to each atom pair.

The GED refinement procedure used for  $\text{Si}_8\text{O}_{12}(\text{CHCH}_2)_8$  allows both  $r_g$ - and  $r_{\text{h}1}$ -type structures to be determined, depending on which distance corrections are applied. The  $r_g$  refinement corrects the distances only along the vector between a given pair of atoms using  $u$ , the root-mean-square amplitude of vibration:

$$r_g = r_a + \frac{u^2}{r_e} \quad (1)$$

where  $r_a$  is the distance ( $\langle r^{-1} \rangle^{-1}$ ) measured by the experiment, and  $r_e$ , the equilibrium distance, is commonly replaced by  $r_a$ . This correction ignores any motion perpendicular to the bond, which can be important. SHRINK<sup>26</sup> allows curvilinear perpendicular correction terms,  $k$ , to be determined from the calculated force constants. When the first-order harmonic approximation is used,  $r_{\text{h}1}$  distances are defined as

$$r_{\text{h}1} = r_a + \frac{u^2}{r_e} - k \quad (2)$$

## RESULTS

**Geometry Optimizations.**  $\text{Si}_8\text{O}_{12}(\text{OSiMe}_3)_8$ . Extensive *ab initio* calculations confirmed that two conformers of  $\text{Si}_8\text{O}_{12}(\text{OSiMe}_3)_8$  exist. The highest-level calculations performed (B3LYP/6-311G\*) showed that the structures lay 1.2 kJ mol<sup>-1</sup> apart in energy, the  $D_4$  conformer being more stable than that with  $D_2$  symmetry. Calculated coordinates are given in the Supporting Information (Table S2). The Boltzmann equation was used to predict the relative abundances of the conformers present in the experiment. The starting point for the GED refinement was therefore chosen with a  $D_4/D_2$  ratio of 0.73:0.27.

The optimized structures of both conformers are shown in Figure 1. In each case, the silicon atoms within the cage host exocyclic OSiMe<sub>3</sub> groups that are bent at the oxygen. The direction of the bend qualitatively describes the orientation of each conformer: the OSiMe<sub>3</sub> groups on each of two opposite faces are all bent in the same sense, thus giving the 4-fold rotation symmetry for the  $D_4$  conformer, while for the  $D_2$  conformer, the OSiMe<sub>3</sub> groups alternate in being bent “up” or “down” with

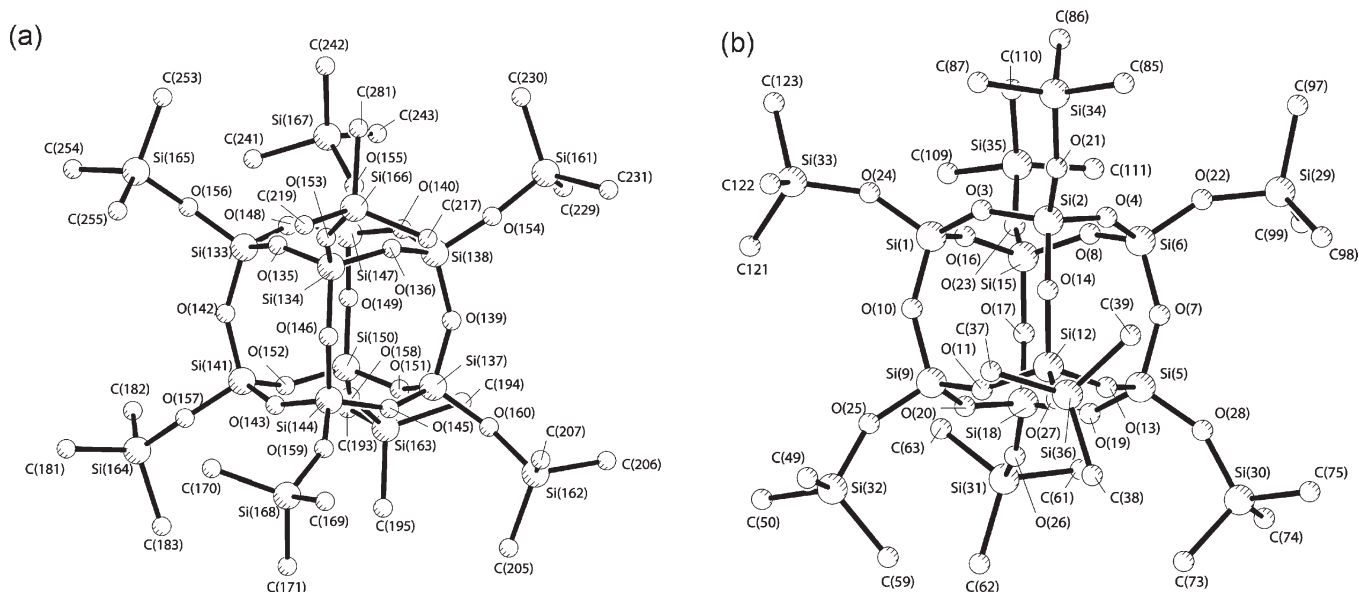


**Figure 1.** Molecular structures of (a) the  $D_4$  conformer and (b) the  $D_2$  conformer of  $\text{Si}_8\text{O}_{12}(\text{OSiMe}_3)_8$  including atom numbering. Hydrogen atoms have been omitted for clarity.

respect to these two faces. Both those groups designated “up” and “down” have OSiC fragments that lie on the mirror planes. Those that are defined as “up” have a dihedral angle formed with the cage oxygen atom that also lies on the mirror plane of  $180^\circ$  [e.g.,  $\text{O}(14)\text{Si}(2)\text{O}(21)\text{Si}(34) = 180^\circ$ ]; the “down” groups have a dihedral angle of  $0^\circ$  [e.g.,  $\text{O}(7)\text{Si}(6)\text{O}(22)\text{Si}(29) = 0^\circ$ ].

$\text{Si}_8\text{O}_{12}(\text{CHCH}_2)_8$ . A potential-energy scan for  $\text{Si}_8\text{O}_{12}\text{H}_7(\text{CHCH}_2)$  was performed with the  $\text{CCSiO}$  dihedral angle set at  $10^\circ$  steps from  $0$  to  $360^\circ$ . All other parameters were allowed to relax at each step. This showed that three minima were present, each relating to a geometry in which a vinyl group eclipses an Si–O bond in the  $\text{Si}_8\text{O}_{12}$  cage. Geometry optimizations were then performed for every isomer of  $\text{Si}_8\text{O}_{12}\text{H}_6(\text{CHCH}_2)_2$ , showing that the relative orientations of two vinyl groups to one another did not significantly affect the total energy of the system. On this basis, it was decided that all possible conformers of  $\text{Si}_8\text{O}_{12}(\text{CHCH}_2)_8$  should be modeled to fit the GED data. The highest symmetry conformer that was calculated had  $D_4$  symmetry, and its Cartesian coordinates are given in Table S3 (Supporting Information). The structure of the  $D_4$  conformer is shown in Figure 2, as is a representation of the model used to describe all possible conformations of  $\text{Si}_8\text{O}_{12}(\text{CHCH}_2)_8$ .

**MD Simulations for  $\text{Si}_8\text{O}_{12}(\text{OSiMe}_3)_8$ .** As was the case for light-atom bonded pairs in previous GED studies of silsesquioxanes,<sup>7–10</sup> the MD method underestimates the C–H amplitudes of vibration because the simulations are performed using classical dynamics. (See ref 9 for a more detailed discussion of this problem.) This results in the neglect of zero-point energy contributions to the thermal motion and prohibits the possibility of quantum-mechanical tunneling. For  $\text{Si}_8\text{O}_{12}\text{Me}_8$ <sup>8,9</sup> and  $\text{Si}_{10}\text{O}_{15}\text{H}_{10}$ ,<sup>10</sup> this was not a substantial problem but resulted in the calculation of C–H and Si–H amplitudes of vibration, respectively, that were about 50% too small. Similar sorts of vibrations and low-frequency oscillations of the OSiMe<sub>3</sub> groups are seen here, and as a result, the C–H amplitudes of vibration have also been underestimated. The starting values used for the GED refinement were therefore taken to be refined values from the  $\text{Si}_6\text{O}_9(\text{OSiMe}_3)_6$  structure.<sup>7</sup> In principle, it is possible to

perform path-integral MD calculations that give accurate vibrational parameters,<sup>9</sup> but they are too resource-intensive to be feasible in this case.

**Distance Corrections for  $\text{Si}_8\text{O}_{12}(\text{CHCH}_2)_8$ .** As mentioned above, force fields were computed to allow perpendicular distance corrections to be determined. It seemed that the only feasible way to obtain these distance corrections for use in the GED refinement would be to calculate them for the  $D_4$  symmetric structure and use these as estimates. However, the high anharmonicity of silsesquioxanes makes the harmonic approximation used to calculate the force constants poor, and it was consequently found that the  $r_{h1}$  refinements (which make use of the perpendicular distance corrections) yielded a poor fit to the experimental data. The low barriers to rotation of the CHCH<sub>2</sub> groups also meant that MD methods such as those for  $\text{Si}_8\text{O}_{12}(\text{OSiMe}_3)_8$  could not be used as unreliable distance corrections, and amplitudes of vibration were predicted, often many magnitudes larger than expected. As any form of anharmonic force constant calculation was also ruled out by the computational resources at our disposal, it was therefore decided that an  $r_g$  refinement (which does not employ perpendicular distance corrections) was most appropriate in this instance. The starting values for the amplitudes of vibration in the GED refinement were taken from the SHRINK<sup>23</sup> using force constants for the  $D_4$ -symmetric conformer.

**GED Refinements.**  $\text{Si}_8\text{O}_{12}(\text{OSiMe}_3)_8$ . A model was written for  $\text{Si}_8\text{O}_{12}(\text{OSiMe}_3)_8$  to allow the refinable geometrical parameters to be converted to Cartesian coordinates. Despite the relatively high symmetries of the two conformers, 62 parameters were required to describe the geometries fully. A full description of the model and a table of parameters (see Table S4) is contained in the Supporting Information. Ultimately, not all parameters were refined, with many subtle differences between similar bond lengths and bond angles fixed at calculated values.

All parameters that described a single bond length, angle, or dihedral angle, or described an overall average, were refined. Flexible SARACEN restraints<sup>31–33</sup> were applied to some parameters that were poorly defined by the GED data, and the smaller

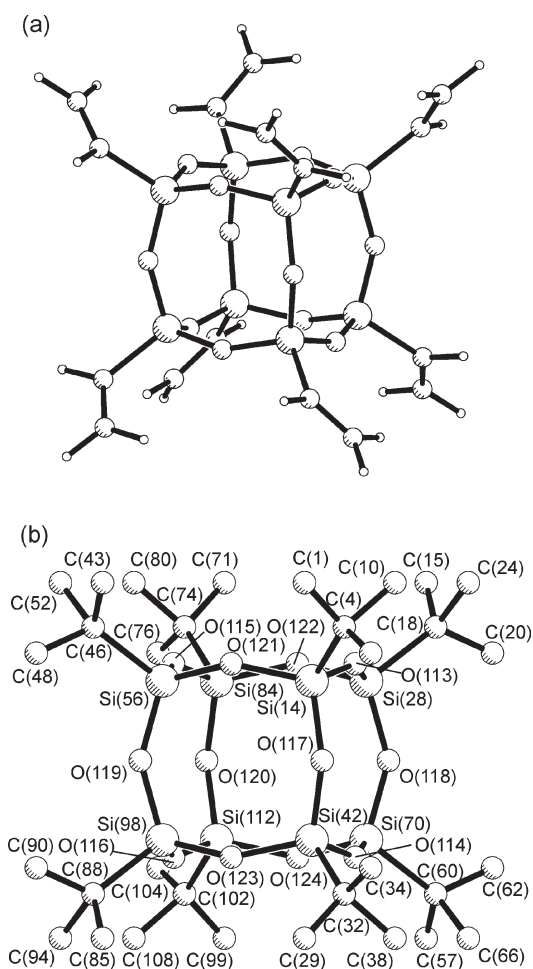


**Figure 2.** (a) Molecular structure of the  $D_4$  conformer of  $\text{Si}_8\text{O}_{12}(\text{CHCH}_2)_8$  and (b) the model used to describe all possible conformations of  $\text{Si}_8\text{O}_{12}(\text{CHCH}_2)_8$ . Hydrogen atoms have been omitted from b for clarity. All terminal carbon atoms are weighted one-third in the GED refinement model.

difference parameters were left unrefined at the values calculated *ab initio*. Restraints had to be applied to some of the difference parameters that were allowed to refine, e.g., parameters relating to the hydrogen-atom positions and a number of dihedral angles and angles relating to the methyl positions. These parameters were restrained to the values obtained from B3LYP/6-311G\* calculations, and their uncertainties were estimated on the basis of the variance of that parameter in different calculations to allow flexibility while restricting nonintuitive refined values. Amplitudes of vibration for distances under the same peak in the radial distribution curve (RDC) were refined by fixing the relative ratios of the amplitudes and then allowing the dominant amplitude to refine. The values for the amplitudes of vibration for the C–H stretches are known to be underestimated as a result of the classical nature of MD simulations. They were therefore started from the refined value obtained in a previous study of  $\text{Si}_6\text{O}_9(\text{OSiMe}_3)_6$ .<sup>7</sup>

A list of the refined value for each parameter ( $r_{e,\text{MD}}$ ), along with its initial theoretical value ( $r_e$ ) and details of any restraint applied, is given in Table S4 (Supporting Information). The abundance of each conformer also affects the  $R_G$  value, and so, once the initial refinement was complete, the fraction of each

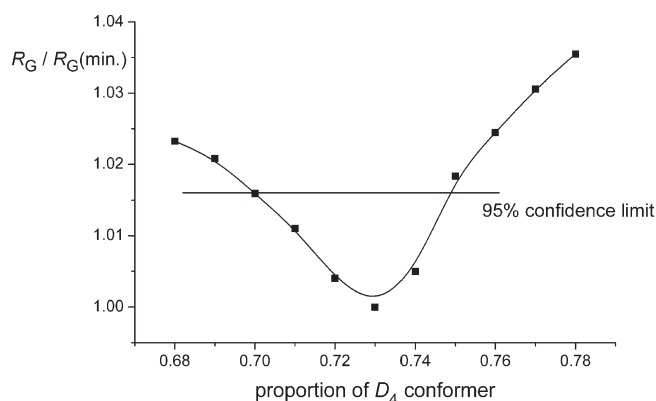


**Figure 3.** Plot of  $R_G / R_G(\text{min})$  for varying proportions of the  $D_4$  conformer.

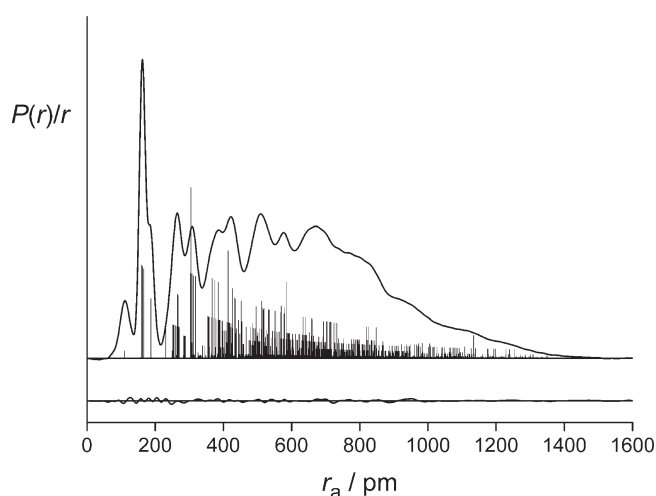


**Figure 4.** Experimental and difference (experimental minus theoretical) radial-distribution curves,  $P(r)/r$ , for  $\text{Si}_8\text{O}_{12}(\text{OSiMe}_3)_8$ . Before Fourier inversion, the data were multiplied by  $s \cdot \exp(-0.00002s^2) / (Z_{\text{Si}} - f_{\text{Si}})(Z_{\text{O}} - f_{\text{O}})$ .

conformer was varied (from the initial state of 0.73  $D_4$  conformer). The abundance of the  $D_4$  conformer was plotted against the resulting  $R_G$  value. From Figure 3, it can be seen that the lowest  $R_G$  value was obtained for an abundance of 0.73 (+0.02/−0.03), indicating that the experiment is in close agreement with the calculations. The values in parentheses are the 95% confidence limits and were estimated using Hamilton's statistical methods.<sup>34</sup>

The final  $R_G$  factor for the fit between the theoretical scattering (generated from the model) and the experimental data for  $\text{Si}_8\text{O}_{12}(\text{OSiMe}_3)_8$  was 0.098 ( $R_D = 0.047$ ). The final radial-distribution and difference curves are shown in Figure 4, and the corresponding molecular-intensity scattering curves are shown in Figure S1 (Supporting Information). A full list of amplitudes of vibration and distance corrections are given in Table S5 (Supporting Information), with the least-squares correlation matrix in Table S6 (Supporting Information) and the final refined Cartesian coordinates in Table S7 (Supporting Information).

$\text{Si}_8\text{O}_{12}(\text{CHCH}_2)_8$ . In order to link the Cartesian coordinates to refinable parameters for  $\text{Si}_8\text{O}_{12}(\text{CHCH}_2)_8$ , a model was written

that accounted for vinyl groups in three possible positions on each silicon atom. A full description of the model and a table of

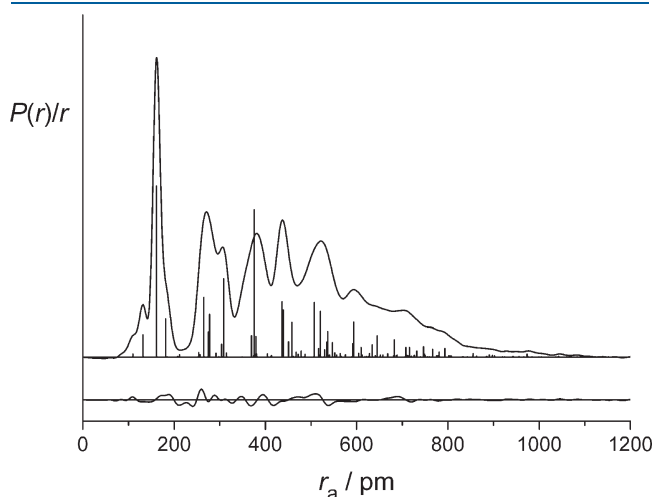


**Figure 5.** Experimental (upper) and final difference (lower, experimental minus theoretical) radial-distribution curves,  $P(r)/r$ , for  $\text{Si}_8\text{O}_{12}(\text{CHCH}_2)_8$ . Before Fourier inversion, the data were multiplied by  $s \cdot \exp(-0.00002s^2)/(Z_{\text{Si}} - f_{\text{Si}})(Z_{\text{O}} - f_{\text{O}})$ .

**Table 1.** Comparison of Average  $r\text{Si}-\text{O}$  Bond Lengths within the Eight-Membered Rings of the Central Frameworks of POSS Structures of the Form  $(\text{RSiO}_{1.5})_n$  as Determined from GED Refinements

$n$	R	$r\text{Si}-\text{O}/\text{pm}$	reference
6	OSiMe <sub>3</sub>	162.35(50)	7
8	H	161.41(3)	8
8	CH <sub>3</sub>	161.74(5)	8
8	CHCH <sub>2</sub>	161.40(9)	this work
8	OSiMe <sub>3</sub>	161.38(8)	this work
10	H	162.2(3)	10

parameters (see Table S8) is contained in the Supporting Information.

The final  $R_G$  factor for the fit between the theoretical scattering (generated from the model) and the experimental data for  $\text{Si}_8\text{O}_{12}(\text{CHCH}_2)_8$  was 0.137 ( $R_D = 0.077$ ). The final radial-distribution and difference curves are shown in Figure 5, and the corresponding molecular-intensity scattering curves are in Figure S2 (Supporting Information). The list of amplitudes of vibration is given in Table S9 (Supporting Information), the least-squares correlation matrix in Table S10 (Supporting Information), and the final refined Cartesian coordinates in Table S11 (Supporting Information).

## DISCUSSION

The structure of  $\text{Si}_8\text{O}_{12}(\text{CHCH}_2)_8$  has been the subject of two crystallographic studies, the first by Baidina et al.,<sup>35</sup> resulting in a final  $R$  factor of 0.11, and the second by Bonhomme et al., with  $R = 0.048$ .<sup>36</sup> In both cases, the vinyl groups were found to be disordered. This is consistent with our calculations, which indicate that the energy differences between the many possible conformers are small. The Si–O distances for Bonhomme et al.'s structure are in the range 159.6(6)–161.6(6) pm, and the Si–O–Si angles range from 150.0(4) to 150.5(4)°. The small ranges for these distances and angles indicate a more symmetrical cage than is often found in crystallographic studies of  $\text{Si}_8\text{O}_{12}$  derivatives. However, given that the vinyl substituents are disordered, the atoms of the cube must also be disordered, at least to some extent, so the atomic coordinates are necessarily averages and must tend toward a more regular cubic structure than for individual molecules. It is not possible, therefore, to deduce anything significant about the extent of deviation from regular cubic symmetry in molecules of  $\text{Si}_8\text{O}_{12}(\text{CHCH}_2)_8$ .

All of the silsesquioxanes studied using GED have some form of eight-membered rings in their structures. Table 1 shows the average oxygen–silicon bond length in the eight-membered rings as determined by GED refinements for these structures. For the molecules with OSiMe<sub>3</sub> ligands based on different central

**Table 2.** Selected Structural Data for  $\text{T}_8\text{R}_8$  Compounds with Oxygen-Centred Substituents<sup>a,b</sup>

R or compound formula	$r\text{Si}-\text{O}$ within $\text{T}_8$ cage		$\angle\text{Si}-\text{O}-\text{Si}$ within $\text{T}_8$ cage		$\angle\text{Si}-\text{O}-\text{X}$ exocyclic		ref
	range	average	range	average	range	average	
–ONMe <sub>4</sub> ·H <sub>2</sub> O	155.8–161.9	159.8	150.03–150.70	150.34			42
–OCu[(H <sub>2</sub> NCH <sub>2</sub> ) <sub>2</sub> ] <sub>2</sub> ·H <sub>2</sub> O	155.9–165.3	161.3	143.17–163.26	150.97			43
–O <sup>−</sup> ·4TMP <sup>c</sup>	157.9–163.2	161.4	148.11–154.69	150.61			44
–ONMe <sub>3</sub> Ph·H <sub>2</sub> O	157.0–163.8	160.7	144.65–156.54	150.12			45
[NMe <sub>3</sub> CH <sub>2</sub> CH <sub>2</sub> OH] <sub>8</sub> [T <sub>8</sub> O <sub>8</sub> ]·24H <sub>2</sub> O	161.4(3)–163.3(3)	162.5	144.70(17)–48.03(17)	146.60			46
–OMe	159.2–160.9	160.4	145.42–151.92	148.15	125.51–128.64	126.7(2)	47
–OSiMe <sub>2</sub> H	159.9(5)–160.7(5)	160.3	148.1–148.3(3)	148.2	159.1(4)	159.1	48
–OSiMe <sub>3</sub>	158.5(9)–161.6(9)	160.0	147.2(6)–150.5(6)	148.8	147.8(7)–156.1(7)	152.0	48
–OSiMe <sub>3</sub> ( $D_4$ isomer)	158.8(4)–161.3(2)	160.5	147.3(9)–150.5(11)	148.9	153.5(9)	153.5	this work
–OSiMe <sub>3</sub> ( $D_2$ isomer)	158.7(4)–164.9(4)	161.4	147.6(10)–148.5(9)	148.1	151.6(9)–152.0(10)	151.8	this work
–OSiMe <sub>2</sub> CH=CH <sub>2</sub>	159.7(3)–160.8(3)	160.2	148.1(3)–148.3(3)	148.2	152.6(2)–153.7(2)	153.2	48
–OSi(CH=CH <sub>2</sub> ) <sub>3</sub>	158.8(3)–161.7(3)	160.8	142.8(2)–151.8(2)	148.5	143.02–151.55	147.06	49
–OSnMe <sub>3</sub>	158.0(3)–162.9(4)	160.8	148.8(2)–161.2(2)	149.3	129.14–140.23	135.49	50
T <sub>8</sub> (OSnMe <sub>3</sub> ) <sub>8</sub> ·4H <sub>2</sub> O	158.72(16)–162.77(17)	161.21	136.35(10)–172.13(12)	149.50	127.15–130.40	128.76	50
T <sub>8</sub> (OTiClCp <sub>2</sub> ) <sub>8</sub> ·3CH <sub>2</sub> Cl <sub>2</sub> <sup>d</sup>	157.9(2)–161.2(2)	160.1	145.36(14)–151.21(16)	148.70	154.22–163.77	158.22	50

<sup>a</sup> Where not supplied in the original publication, data have been derived from the relevant structure in the Cambridge Crystallographic Database.

<sup>b</sup> Distances ( $r$ ) are in pm; angles ( $\angle$ ) are in degrees. <sup>c</sup> TMP = 1,1,4,4-tetramethylpiperazinium. <sup>d</sup> Cp = cyclopentadienyl.

cage structures, the average Si–O bond length is seen to increase slightly with the decreasing number of atoms in the central cage: 161.38(8) pm for  $\text{Si}_8\text{O}_{12}(\text{OSiMe}_3)_8$  and 162.35(50) pm for  $\text{Si}_6\text{O}_9(\text{OSiMe}_3)_6$ . The difference of 1 pm can be attributed to the different overall shapes of the internal silicon–oxygen frameworks. The six-membered cap rings in  $\text{Si}_6\text{O}_9(\text{OSiMe}_3)_6$  force the structure closer together than the eight-membered cap rings in  $\text{Si}_8\text{O}_{12}(\text{OSiMe}_3)_8$ , and so the Si–O bond lengths in the smaller structure increase to compensate.

When comparing the two compounds with  $\text{R} = \text{H}$  ( $\text{Si}_8\text{O}_{12}\text{H}_8$  and  $\text{Si}_{10}\text{O}_{15}\text{H}_{10}$ ), we see a similar trend, with the average eight-membered ring Si–O bond length increasing from 161.41(3) to 162.2(3) pm in the compound that also contains larger 10-membered rings. In the original analysis, it was concluded that the 10-membered rings are exceptionally flexible, and thus the extended vibrations cause a stretching of the bond.<sup>10</sup>

To analyze the effect of varying the substituent, the average bond lengths within structures with  $n = 8$  are compared in Table 1. In this case, it can be observed that the average Si–O bond length increases with the electron-donating properties of the substituents. The methyl group in  $\text{Si}_8\text{O}_{12}\text{Me}_8$  is an electron-donating group, which therefore reduces the positive charge on silicon and so lengthens the Si–O bond. Conversely, in  $\text{Si}_8\text{O}_{12}(\text{OSiMe}_3)_8$ , the oxygen that binds the substituent to the cage is electron-withdrawing and therefore increases the positive charge on the cage silicon, which in turn attracts the bonded oxygen atoms within the cube, and the average Si–O bond is shortened.

Clearly the structures of such molecules are determined by a wide range of interactions and influences. To account for and understand the variations further is a challenge for future studies. Once a larger variety of POSS structures has been studied, both with different substituents and various cage sizes, the underlying nuances may start to be fully understood.

The near cubic arrangement of main-group elements bridged by oxygen atoms, as in  $[\text{Si}_8\text{O}_{20}]^{8-}$ , is a well-known structural building unit in zeolite chemistry,<sup>37,38</sup> where it is usually called the double-four ring (D4R). This type of building unit can also be found in many other three-dimensional frameworks as well as in sheets, chains, and discrete molecular structures.<sup>39</sup> The sequential reaction of  $[\text{Si}_8\text{O}_{20}]^{8-}$  with  $(\text{EtO})_3\text{SiCl}$  and  $\text{Me}_3\text{SiCl}$  to give  $\text{Si}_8\text{O}_{12}[\text{OSi}(\text{OSiMe}_3)_3]_8$  provides a bottom-up approach to well-defined silica nanoparticles containing a  $[\text{Si}_8\text{O}_{20}]^{8-}$  core.<sup>40</sup> A direct comparison of the structure of  $\text{Si}_8\text{O}_{12}(\text{OSiMe}_3)_8$  with that of zeolite D4R cages is difficult, because of the presence of both Al and Si in the zeolite cages, and the presence of cations, such as Na, that can sit over some of the faces of the polyhedra, thus distorting them. However, the structure of dehydrated zeolite A, for example, has T–O–T (where T may be Si or Al) angles of 142.2(2) and 144.8(1)° within the cage and a T–O–T angle of 164.7(2)° linking the cages<sup>41</sup> compared with 147.3(9) and 150.5(11)° (cage Si–O–Si) and 153.5(9)° (ligand Si–O–Si) in the  $D_4$  conformer of  $\text{Si}_8\text{O}_{12}(\text{OSiMe}_3)_8$ . Table 2 shows structural data for a range of compounds containing an  $\text{Si}_8\text{O}_{12}$  core with O-connected substituents. As can be seen, the range of Si–O bond lengths within the cages is small, and although the Si–O–Si angles within the cages may vary significantly, the range of the averages is also small. A comparison of the ranges of Si–O–Si angles within the cage and the Si–O–X exocyclic angles shows that they are similar within a particular molecule, despite the Si–O–Si endocyclic linkages being held as part of a cage. This is consistent with the previously noted flexibility of  $\text{Si}_8\text{O}_{12}$  cages.<sup>1,2</sup>

## ■ ASSOCIATED CONTENT

**S Supporting Information.** Experimental parameters for the GED analyses of  $\text{Si}_8\text{O}_{12}(\text{OSiMe}_3)_8$  and  $\text{Si}_8\text{O}_{12}(\text{CHCH}_2)_8$  (Table S1), calculated Cartesian coordinates for  $\text{Si}_8\text{O}_{12}(\text{OSiMe}_3)_8$  (Table S2), calculated Cartesian coordinates for the  $D_4$  conformer of  $\text{Si}_8\text{O}_{12}(\text{CHCH}_2)_8$  (Table S3), model description for  $\text{Si}_8\text{O}_{12}(\text{OSiMe}_3)_8$  (Table S4), refined and calculated RMS amplitudes of vibration and corresponding distance corrections for  $\text{Si}_8\text{O}_{12}(\text{OSiMe}_3)_8$  (Table S5), least-squares correlation matrix for the GED refinement of  $\text{Si}_8\text{O}_{12}(\text{OSiMe}_3)_8$  (Table S6), final refined Cartesian coordinates for  $\text{Si}_8\text{O}_{12}(\text{OSiMe}_3)_8$  (Table S7), model description for  $\text{Si}_8\text{O}_{12}(\text{CHCH}_2)_8$  (Table S8), refined and calculated amplitudes of vibration for  $\text{Si}_8\text{O}_{12}(\text{CHCH}_2)_8$  (Table S9), least-squares correlation matrix for the GED refinement of  $\text{Si}_8\text{O}_{12}(\text{CHCH}_2)_8$  (Table S10), final refined Cartesian coordinates for  $\text{Si}_8\text{O}_{12}(\text{CHCH}_2)_8$  (Table S11), molecular-intensity scattering and difference curves for  $\text{Si}_8\text{O}_{12}(\text{OSiMe}_3)_8$  (Figure S1), and molecular-intensity scattering and difference curves for  $\text{Si}_8\text{O}_{12}(\text{CHCH}_2)_8$  (Figure S2). This material is available free of charge via the Internet at <http://pubs.acs.org>.

## ■ AUTHOR INFORMATION

### Corresponding Author

\*E-mail: [derek.wann@ed.ac.uk](mailto:derek.wann@ed.ac.uk) (D.A.W.), [p.lickiss@imperial.ac.uk](mailto:p.lickiss@imperial.ac.uk) (P.D.L.).

## ■ ACKNOWLEDGMENT

The EPSRC is acknowledged for funding the electron-diffraction research in Edinburgh (EP/C513649). The EaStCHEM RCF and NSCCS provided valuable computational hardware and software support.

## ■ REFERENCES

- (1) Lickiss, P. D.; Rataboul, F. *Adv. Organomet. Chem.* **2008**, *57*, 1.
- (2) Cordes, D. B.; Lickiss, P. D.; Rataboul, F. *Chem. Rev.* **2010**, *110*, 2081.
- (3) Quadrelli, E. A.; Basset, J.-M. *Coord. Chem. Rev.* **2010**, *254*, 707.
- (4) Di Iulio, C.; Jones, M. D.; Mahon, M. F.; Apperley, D. C. *Inorg. Chem.* **2010**, *49*, 10232.
- (5) Duchateau, R. *Chem. Rev.* **2002**, *102*, 3525.
- (6) Laine, R. M.; Sulaiman, S.; Brick, C.; Roll, M.; Tamaki, R.; Asuncion, M. Z.; Neurock, M.; Filhol, J.-S.; Lee, C.-Y.; Zhang, J.; Goodson, T.; Ronchi, M.; Pizzotti, M.; Rand, S. C.; Li, Y. *J. Am. Chem. Soc.* **2010**, *132*, 3708.
- (7) Wann, D. A.; Reilly, A. M.; Rataboul, F.; Lickiss, P. D.; Rankin, D. W. H. *Z. Naturforsch. B* **2009**, *64*, 1269.
- (8) Wann, D. A.; Less, R. J.; Rataboul, F.; McCaffrey, P. D.; Reilly, A. M.; Robertson, H. E.; Lickiss, P. D.; Rankin, D. W. H. *Organometallics* **2008**, *27*, 4183.
- (9) Wann, D. A.; Zakharov, A. V.; Reilly, A. M.; McCaffrey, P. D.; Rankin, D. W. H. *J. Phys. Chem. A* **2009**, *113*, 9511.
- (10) Wann, D. A.; Rataboul, F.; Reilly, A. M.; Robertson, H. E.; Lickiss, P. D.; Rankin, D. W. H. *Dalton Trans.* **2009**, 6843.
- (11) Agaskar, P. A. *Inorg. Chem.* **1990**, *29*, 1603.
- (12) Gao, J.-G.; Wang, S.-C.; Zhang, X.-J.; Run, M.-T. *Youjigui Cailiao* **2005**, *19*, 5.
- (13) Frisch, M. J.; Trucks, G. W.; Schlegel, H. B.; Scuseria, G. E.; Robb, M. A.; Cheeseman, J. R.; Montgomery, J. A., Jr.; Vreven, T.; Kudin, K. N.; Burant, J. C.; Millam, J. M.; Iyengar, S. S.; Tomasi, J.; Barone, V.; Mennucci, B.; Cossi, M.; Scalmani, G.; Rega, N.; Petersson,

- G. A.; Nakatsuji, H.; Hada, M.; Ehara, M.; Toyota, K.; Fukuda, R.; Hasegawa, J.; Ishida, M.; Nakajima, T.; Honda, Y.; Kitao, O.; Nakai, H.; Klene, M.; Li, X.; Knox, J. E.; Hratchian, H. P.; Cross, J. B.; Adamo, C.; Jaramillo, J.; Gomperts, R.; Stratmann, R. E.; Yazyev, O.; Austin, A. J.; Cammi, R.; Pomelli, C.; Ochterski, J. W.; Ayala, P. Y.; Morokuma, K.; Voth, G. A.; Salvador, P.; Dannenberg, J. J.; Zakrzewski, V. G.; Dapprich, S.; Daniels, A. D.; Strain, M. C.; Farkas, O.; Malick, D. K.; Rabuck, A. D.; Raghavachari, K.; Foresman, J. B.; Ortiz, J. V.; Cui, Q.; Baboul, A. G.; Clifford, S.; Cioslowski, J.; Stefanov, B. B.; Liu, G.; Liashenko, A.; Piskorz, P.; Komaromi, I.; Martin, R. L.; Fox, D. J.; Keith, T.; Al-Laham, M. A.; Peng, C. Y.; Nanayakkara, A.; Challacombe, M.; Gill, P. M. W.; Johnson, B.; Chen, W.; Wong, M. W.; Gonzalez, C.; Pople, J. A. *Gaussian 03*, revision C.02; Gaussian, Inc.: Wallingford, CT, 2004.
- (14) National Service for Computational Chemistry Software (NSCCS). <http://www.nscs.ac.uk> (accessed Mar 2011).
- (15) Krishnan, R.; Frisch, M. J.; Pople, J. A. *J. Chem. Phys.* **1980**, *72*, 4244.
- (16) McLean, A. D.; Chandler, G. S. *J. Chem. Phys.* **1980**, *72*, 5639.
- (17) Becke, A. D. *J. Chem. Phys.* **1993**, *98*, 5648.
- (18) Lee, C.; Yang, W.; Parr, R. G. *Phys. Rev. B* **1992**, *37*, 785.
- (19) Miehl, B.; Savin, A.; Stoll, H.; Preuss, H. *Chem. Phys. Lett.* **1989**, *157*, 200.
- (20) Stewart, J. J. P. *J. Mol. Model.* **2007**, *13*, 1173.
- (21) Thiel, W. A.; Voityuk, A. *Theor. Chim. Acta* **1992**, *81*, 391.
- (22) VandeVondele, J.; Krack, M.; Mohamed, F.; Parrinello, M.; Chassaing, T.; Hutter, J. *Comput. Phys. Commun.* **2005**, *167*, 103.
- (23) EaStCHEM Research Computing Facility (<http://www.east-chem.ac.uk/rcf>). This facility is partially supported by the eDIKT initiative (<http://www.edikt.org>).
- (24) Bussi, G.; Donadio, D.; Parrinello, M. *J. Chem. Phys.* **2007**, *126*, 014101.
- (25) Zakharov, A. V. Personal communication.
- (26) Sipachev, V. A. *THEOCHEM* **1985**, *121*, 143. Sipachev, V. A. *J. Mol. Struct.* **2001**, *567*, 67.
- (27) Huntley, C. M.; Laurensen, G. S.; Rankin, D. W. H. *J. Chem. Soc., Dalton Trans.* **1980**, 954.
- (28) Fleischer, H.; Wann, D. A.; Hinchley, S. L.; Borisenko, K. B.; Lewis, J. R.; Mawhorter, R. J.; Robertson, H. E.; Rankin, D. W. H. *Dalton Trans.* **2005**, 3221.
- (29) Hinchley, S. L.; Robertson, H. E.; Borisenko, K. B.; Turner, A. R.; Johnston, B. F.; Rankin, D. W. H.; Ahmadian, M.; Jones, J. N.; Cowley, A. H. *Dalton Trans.* **2004**, 2469.
- (30) Ross, A. W.; Fink, M.; Hilderbrandt, R. In *International Tables for Crystallography*; Wilson, A. J. C., Ed.; Kluwer Academic Publishers: Dordrecht, The Netherlands, 1992; Vol. C, p 245.
- (31) Blake, A. J.; Brain, P. T.; McNab, H.; Miller, J.; Morrison, C. A.; Parsons, S.; Rankin, D. W. H.; Robertson, H. E.; Smart, B. A. *J. Phys. Chem.* **1996**, *100*, 12280.
- (32) Brain, P. T.; Morrison, C. A.; Parsons, S.; Rankin, D. W. H. *J. Chem. Soc., Dalton Trans.* **1996**, 4589.
- (33) Mitzel, N. W.; Rankin, D. W. H. *Dalton Trans.* **2003**, 3650.
- (34) Hamilton, W. C. *Acta Crystallogr.* **1965**, *18*, 502.
- (35) Baidina, I. A.; Podberezskaya, N. V.; Alekseev, V. I.; Martynova, T. N.; Borisov, S. V.; Kanev, A. N. *J. Struct. Chem.* **1980**, *20*, 550.
- (36) Bonhomme, C.; Tolédano, P.; Maquet, J.; Livage, J.; Bonhomme-Coury, L. *J. Chem. Soc., Dalton Trans.* **1997**, 1617.
- (37) Meier, W. M.; Olson, D. H.; Baerlocher, C. *Atlas of Zeolite Types*; Elsevier: London, 1996.
- (38) The International Zeolite Association Structure Commission (see <http://www.iza-structure.org>).
- (39) See: Mellot-Draznieks, C.; Girard, S.; Férey, G. *J. Am. Chem. Soc.* **2002**, *124*, 15326 for a discussion of possible structures.
- (40) Kawahara, K.; Hagiwara, Y.; Shimojima, A.; Kuroda, K. *J. Mater. Chem.* **2008**, *18*, 3193.
- (41) Pluth, J. J.; Smith, J. V. *J. Am. Chem. Soc.* **1980**, *102*, 4704.
- (42) Smolin, Yu. I.; Shepelev, Yu. F.; Pomes, R.; Hoebbel, D. *Kristallografiya* **1979**, *24*, 38.
- (43) Smolin, Yu. I.; Shepelev, Yu. F.; Butikova, I. K. *Kristallografiya* **1972**, *17*, 15.
- (44) Wiebcke, M.; Emmer, J.; Felsche, J.; Hoebbel, D.; Engelhardt, G. *Z. Anorg. Allg. Chem.* **1994**, *620*, 757.
- (45) Emmer, J.; Wiebcke, M. *J. Chem. Soc., Chem. Commun.* **1994**, 2079.
- (46) Asuncion, M. Z.; Hasegawa, I.; Kampf, J. W.; Laine, R. M. *J. Mater. Chem.* **2005**, *15*, 2114.
- (47) Day, V. W.; Klemperer, W. G.; Mainz, V. V.; Millar, D. M. *J. Am. Chem. Soc.* **1985**, *107*, 8262.
- (48) Auner, N.; Ziemer, B.; Herrschaft, B.; Ziche, W.; John, P.; Weis, J. *Eur. J. Inorg. Chem.* **1999**, *7*, 1087.
- (49) Slebodnick, C.; Angel, R. J.; Hanson, B. E.; Agaskar, P. A.; Soler, T.; Falvello, L. R. *Acta Crystallogr., Sect. B: Struct. Sci.* **2008**, *64*, 330.
- (50) Clark, J. C.; Saengerkerdsub, S.; Eldridge, G. T.; Campana, C.; Barnes, C. E. *J. Organomet. Chem.* **2006**, *691*, 3213.